Electronic Supplementary Material (ESI) for Energy & Environmental Science

Supporting Information

High-Performance hybrid plastic films: A robust electrode platform for thin-film optoelectronics

Jungho Jin,‡ Jaemin Lee,‡ Seonju Jeong, SeungCheol Yang, Ji-Hoon Ko, Hyeon-Gyun Im, Se-Woong Baek, Jung-Yong Lee,* and Byeong-Soo Bae*

1. Fabrication and thermo-mechanical /thermal analyses of GFRHybrimer films

The base GFRHybrimer film can be fabricated by a series of procedures described elsewhere.[1] Briefly, two sheets of E-glass fabric (25 μm) were placed on a pre-cleaned glass plate and subsequently impregnated with the hybrimer resin (Figure S4). The sample was then covered with another glass plate and pressed in a vacuum bag molding instrument. After UV-curing the sample, a transparent GFRHybrimer film can be obtained by separating the two glasses. Based on our rough calculations, the cost to produce a GFRhybrimer film including glass fabrics (10 x 10 cm^2 in size) is approximately \$1.80/sheet,[2] and the cost of AgNW ink (20 Ω/sq) is \$0.08/sheet. Moreover, the ITO/PEN substrates, which we used for comparison with AgNW-GFRHybrimer films, cost \$78/sheet (10 x 10 cm^2 in size).[3] We strongly believe that actual cost for mass productions of our film would be significantly reduced and the cost-competitiveness of our AgNW-GFRHybrimer film would be also attractive for implementation of less expensive organic solar cells.

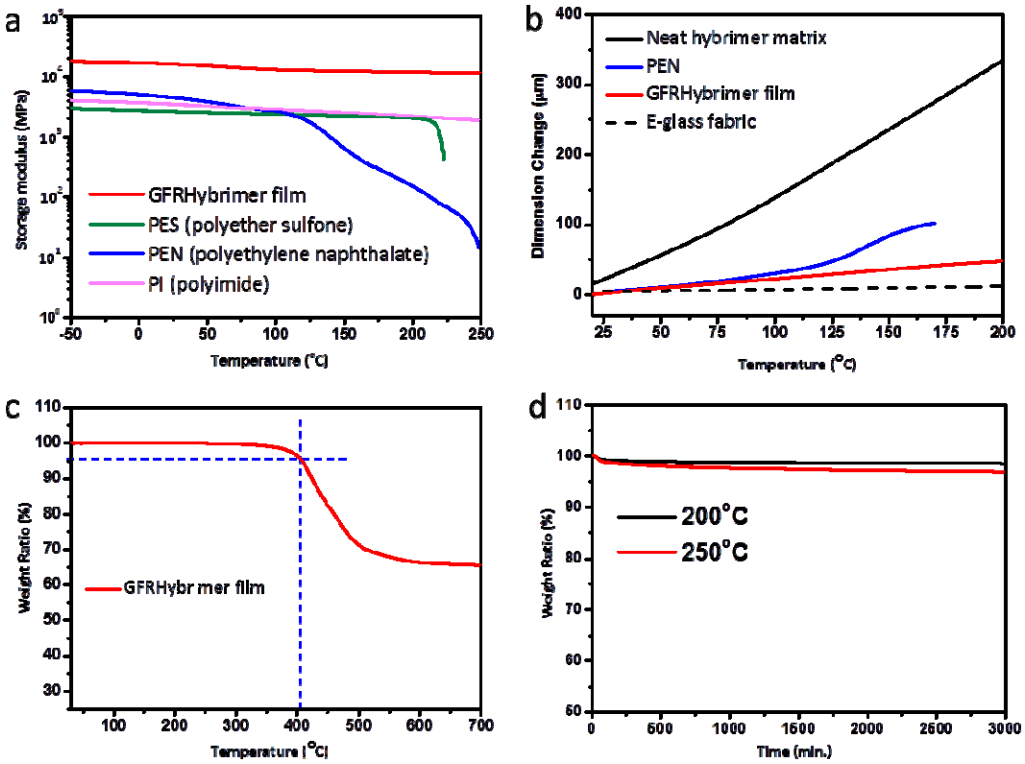

Figure S1. Thermo-mechanical and thermal analyses of GFRHybrimer films. (a) Dynamic mechanical analysis (DMA) of GFRHybrimer film, PES (polyethersulfone), PEN (polyethylene naphthalate), and PI (polyimide). The storage modulus of the GFRHybrimer film remains ~10 GPa over a temperature range from -50 to 250 °C, which is higher than that of typical plastic films. (b) Thermo-mechanical analysis (TMA) of a neat hybrimer matrix, GFRHybrimer film, PEN, and E-glass fabric. The CTE of the GFRHybrimer film was ~15 ppm/°C (optimal value) without exhibiting any glass transition behavior, while the PEN film shows an abrupt increase in CTE at its glass transition temperature. The CTE of the GFRHybrimer is dependent on the total thickness of the film and can be altered by controlling vacuum bag molding process parameters such as temperature, vacuum time, and pressure. (c) Thermo-gravimetric analysis (TGA) of GFRHybrimer film (in N_2). Note that the 5 % weight-loss temperature of the GFRHybrimer film exceeds 400 °C. (d) Isothermal TGA analysis of GFRHybrimer film at 200 °C and 250 °C (in N_2).

2. Dimensions of synthesized AgNWs

The AgNWs were synthesized by a modified polyol process.[4] The synthesized AgNWs had diameter and length of ca. 70.3 nm and 11 μm, respectively. The length and the diameter of

the AgNWs were assessed from a SEM analysis, as shown in the inset of Figure S2a and S2b. Both figures illustrate histograms of wire dimensions. Figure S2c reveals the formation of networks between wires after spraying without annealing. By annealing the networks at 250 °C for 20 mins, the NW-NW junctions were more strongly secured, as shown in the Figure S2d, and, as a result, the sheet resistance of the film decreases.

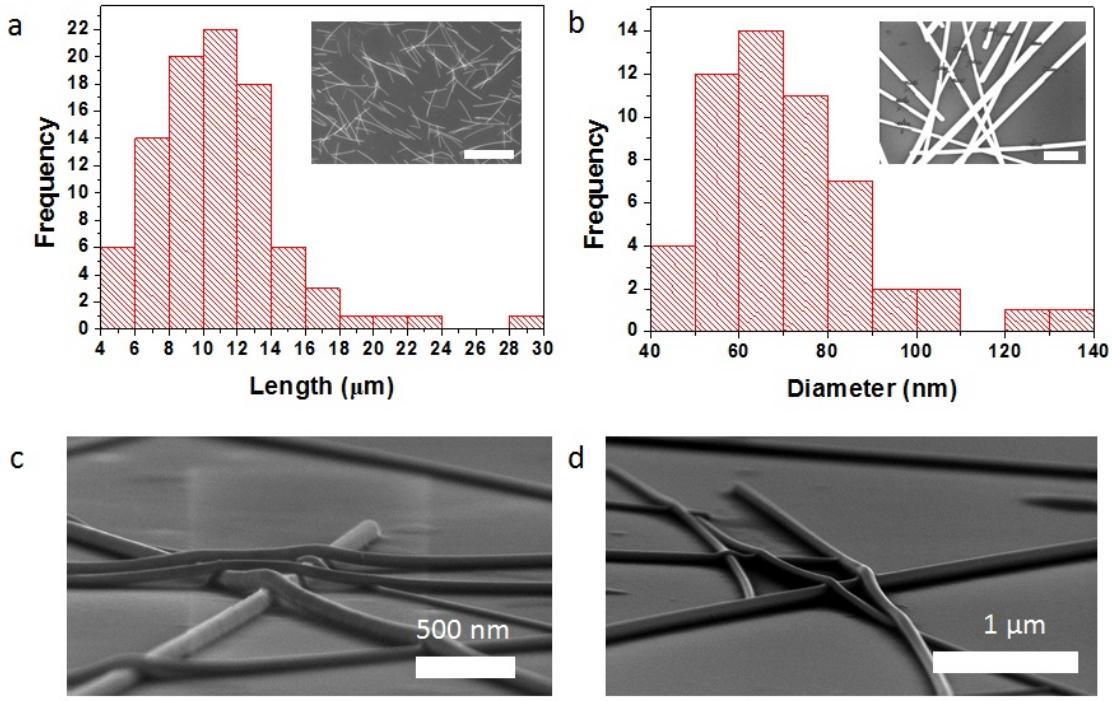

Figure S2. Histograms and SEM images of the synthesized AgNWs. (a) Histogram of length of AgNWs. (b) Histogram of diameter of AgNWs. For (a) and (b), The magnified SEM image of AgNWs in the inset shows the distribution of diameters of AgNWs. The scale bars are 10 μm and 500 nm, respectively. (c) SEM image of as-spray-deposited AgNWs. (d) SEM image of the AgNWs after heat-treatment at 250 °C.

3. Automated spray system for large-area deposition of AgNWs

To prepare AgNW random meshes on a glass substrate (Figure 1, step I), a suspension of AgNWs was deposited on a pre-cleaned soda-lime glass with the aid of an automated spray system, as shown in Figure S3a. The spray system consists of an automated moving atomic nozzle (internal mixture type) along the x and y axes, a syringe pump and suspension inlet, a

pressure gas inlet, a z-axis movable hotplate, a spray booth made of acryl for consistent atmosphere and moisture, and an exhaust line. All the deposition conditions were optimized to secure highly transparent and conductive AgNW electrodes. The spray process involves a number of parameters that influence the morphology of the deposited AgNWs, such as scan speed, nozzle-to-substrate distance, AgNW solution concentration, flow rate, back pressure, substrate hydrophobicity, and substrate temperature. We optimized a set of process conditions that enables uniform distribution of AgNWs (Figure S3b and Experimental Section). Otherwise, spray deposition of AgNWs under non-optimal process conditions yielded undesirable agglomerations of AgNWs, as shown in Figure S3c. Generally, the spraying temperature, suspension flow rate, and pressure to the nozzle are the most important factors to prevent the deposition of non-uniformly distributed AgNWs.[5] It is important to secure a uniform distribution of AgNWs as it is directly related to the opto-electrical performance of the AgNW electrode in terms of the T- R_{sh} relation. The spray-coated (*i.e.*, pre-formed) AgNWs were then annealed at 250 °C for 20 min, resulting in an effective decrease in R_{sh} due to fusion of AgNWs, as anticipated (Figure S2d).

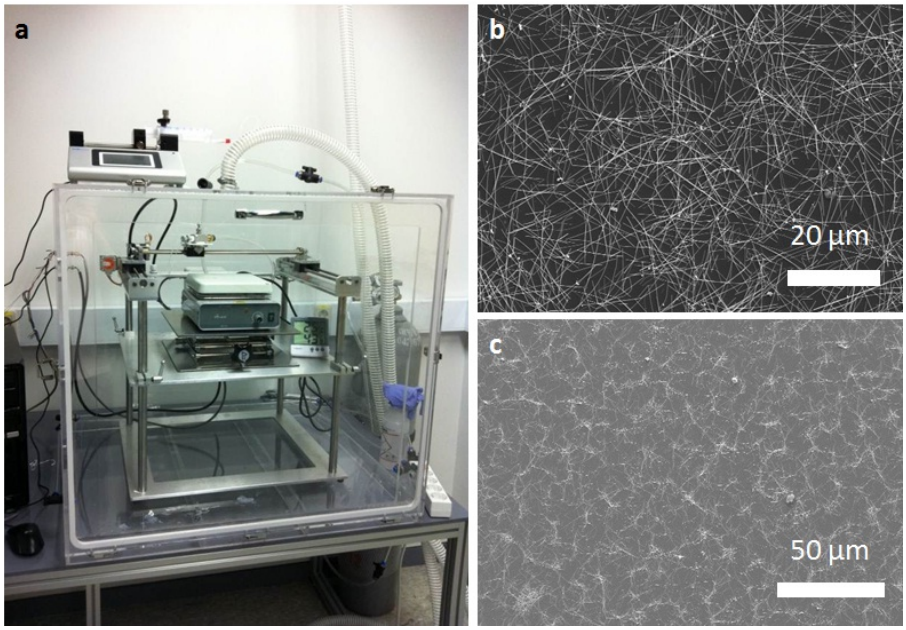

Figure S3. Automated spray deposition system and AgNW networks. (a) Large-area spray deposition system. (b) Uniform distribution of AgNWs deposited by the optimal spray conditions. (c) Agglomeration of AgNWs deposited by non-optimal spray conditions. The agglomerations are unfavorable for collection or injection of carriers in optoelectronic devices.

4. Chemical structure of materials comprising the matrix for the AgNW-GFRHybrimer film

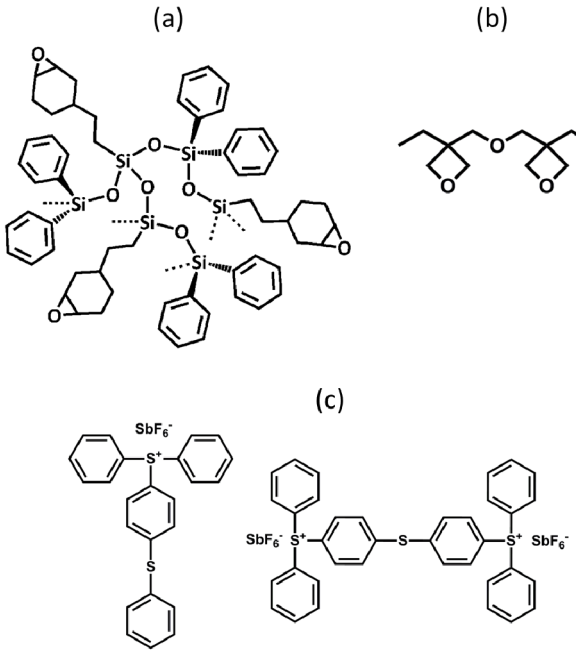

Figure S4. Chemical structure of materials comprising the matrix for the AgNW-GFRHybrimer film. (a) Cyclo-aliphatic epoxy hybrid material (base resin). (b) Bis[1-ethyl(3-oxetanyl)]methyl ether (cross-linker). (c) Triarylsulfonium hexafluoroantimonate salt (cationic photo-initiator).

5. Effect of suspension purification on the transfer of AgNWs

Adhesion between AgNWs and the donor glass substrate also plays a critical role in the transfer process of the AgNWs to the GFRHybrimer. This is particularly true when the adhesion is undesirably strong; in this case, we observed scattering of un-transferred AgNWs left on the original donor glass substrate after the transfer. We found that the strong adhesion was mostly caused by organic residues such as PVP in the AgNW suspension and can be

resolved by using a purified AgNW suspension through careful washing. Figure S5 demonstrates the transfer processes with properly purified and unpurified AgNW suspensions. With proper washing of AgNWs to remove the organic residues, we could easily detach the AgNWs with 3M scotch tape, as shown in Figure S5a, revealing weak adhesion of the AgNWs to the substrate. Consequently, almost all the AgNWs were transferred easily onto the GFRHybrimer film and few AgNWs were found on the donor glass substrate, as shown in Figure S5b and S5c, compared to the pre-formed AgNW film on the donor substrate (Figure S5d). However, if the AgNW suspension was not properly washed, it was difficult to detach the AgNWs with tape (Figure S5e) and AgNWs remained on the donor glass substrate, as observed in Figure S5f and S5g.

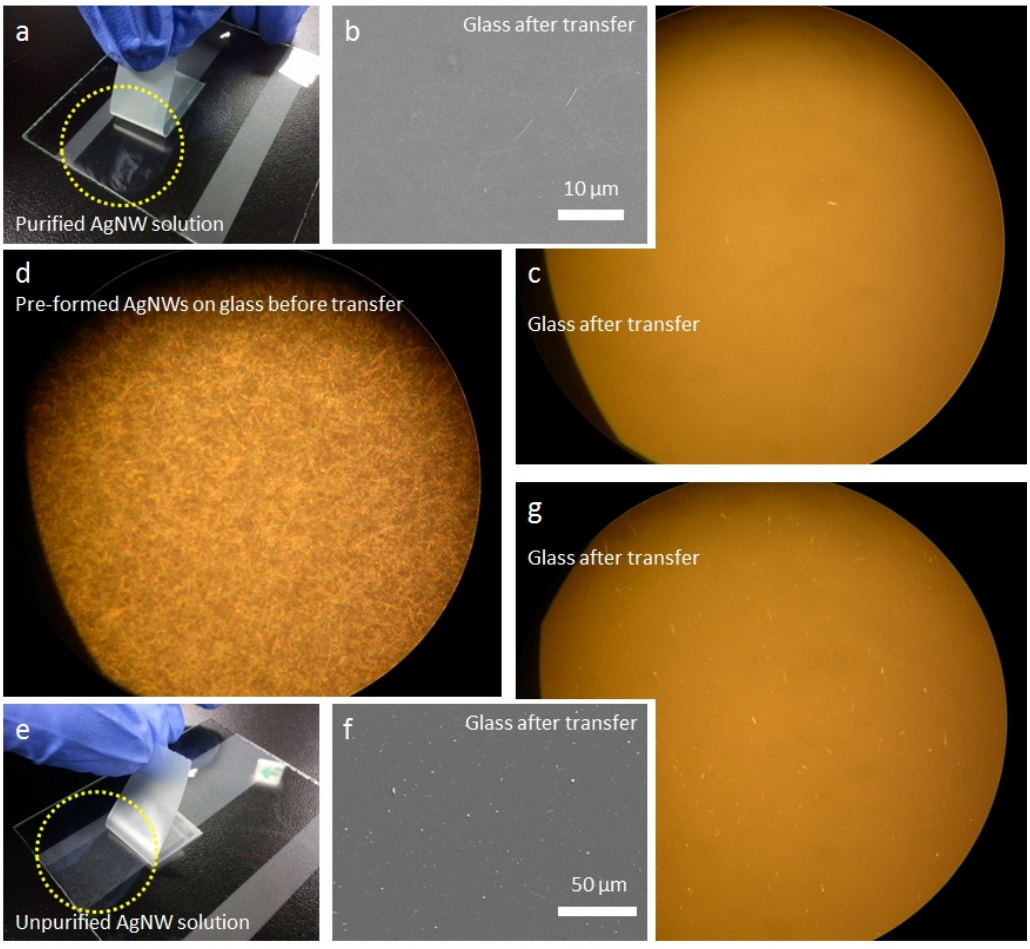

Figure S5. Transfer of AgNWs with purified and unpurified AgNW suspensions. (a) Adhesion test with 3M tape. We could easily detach purified AgNWs. (b), (c) SEM and optical microscope images of the donor glass substrate after transfer. We found very few AgNWs remaining on the glass. (d) The pre-formed AgNW networks on glass before transfer. (e) The unpurified AgNWs were not fully removed by 3M tape. (f), (g) SEM and optical microscope images of the donor glass substrate after transfer. Note that scattering of un-transferred AgNWs is observed in the case of unpurified AgNWs.

6. Mechanical abrasion resistance of the Ag-GFRHybrimer film

To investigate the mechanical abrasion resistance of the AgNW-GFRHybrimer, we performed abrasion tests with the 3M tape and eraser, as depicted in Figure S6a and S6b. The tape was fully adhered on the AgNW-GFRHybrimer film and then detached after a few minutes. In the case of the tape test, we could not find any increase in the sheet resistance after repeated attach-detach cycles. For the eraser test, we rubbed the film a few times, and the sheet resistance was increased by only 1.4 Ω/sq. (Figure S6c and the inset) Although the same tests were repeated, there was extremely little further degradation, implying that the AgNWs were securely embedded in the GFRHybrimer substrate and resistant to mechanical abrasion.

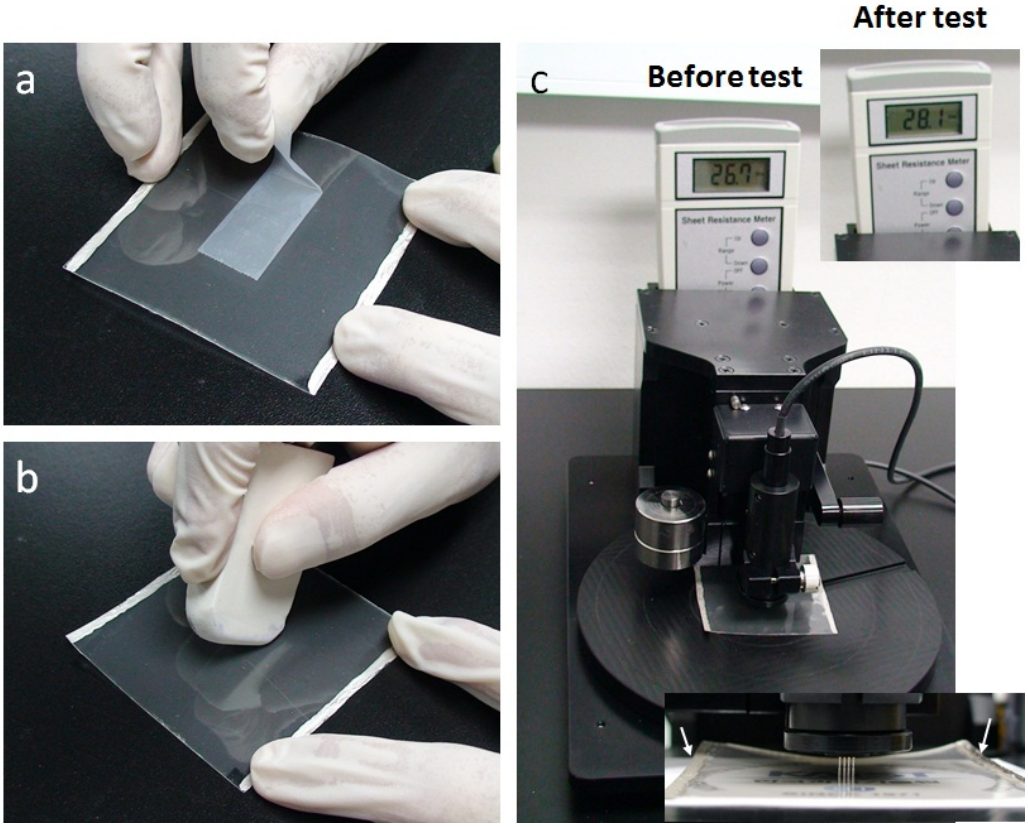

Figure S6. Mechanical abrasion stability test of AgNW-GFRHybrimer film. (a) 3M tape test. (b) Eraser test. (c) The R_{sh} measurement before and after both tests using a 4-point probe system. The inset at the bottom shows the tip contact on the AgNW-GFRHybrimer surface. The white arrows indicate the aluminum pads to measure the sheet resistance with a multimeter for crosschecking. We confirmed that the sheet resistances by both methods are almost identical.

7. Stability test of the inverted OSCs on AgNW-GFRHybrimer film

The inverted OSC on the AgNW-GFRHybrimer showed relatively good stability both in air and N_2 under ambient conditions. Figure S7 illustrates the normalized power conversion efficiency (PCE) of the devices evaluated *in air* under 100 mW/cm^2 AM1.5 illumination, while the devices were stored in a nitrogen-filled glove box and air for 600h. The power conversion efficiencies (PCEs) of the devices stored in nitrogen and air for 25 days were approximately 60 % and 40 % of the initial PCEs, respectively. The air stability of the

inverted OSC on the AgNW-GFRHybrimer film is reasonable,[6,7] considering that it has been stored in hot (~30 °C) and humid (60~70 % RH) conditions.

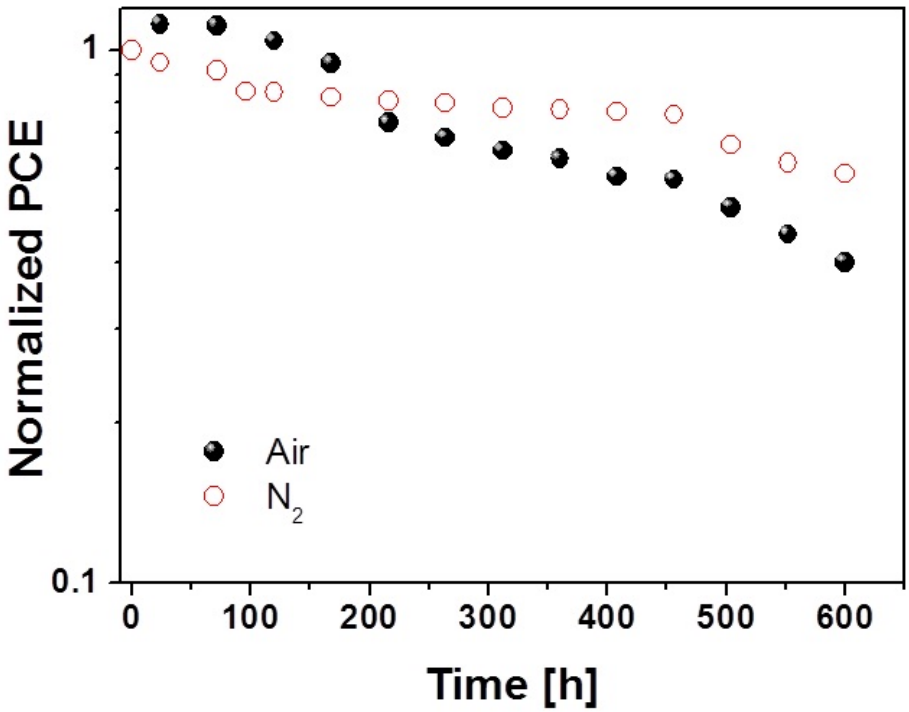

Figure S7. Stability of the inverted OSCs on AgNW-GFRHybrimer film. Power conversion efficiency, normalized to the initial values, for non-passivated inverted OSCs on the AgNW-GFRHybrimer as a function of exposure time to ambient air (filled circle) and N_2 (empty circle) under 100 mW/cm^2 AM1.5 illumination.

Table S1. Total optical transmittance (λ= 550nm) of AgNW-GFRHybrimer films with various sheet resistances with respect to air and GFRHybrimer film.

	Baseline	15 Ω/sq	22 Ω/sq	200 Ω/sq	GFRHybrimer
T (%) (@ 550 nm wavelength)	Ambient air	81.8	85.0	86.7	90.6
	GFRHybrimer	90.4	94.1	96.0	-

Table S2. Reduction of the R_{sh} of AgNW-GFRHybrimer film after transfer.

Before transfer [Ω/sq]	After transfer [Ω/sq]
24	22
18	16.5
11.1	9.2

Table S3. Shore-D values of common plastic films and GFRHybrimer film. A higher Shore-D value is advantageous in grasping the AgNWs tightly during the transfer process and various post-treatments.

Films	PDMS	Poly acrylate	PEN	GFRHybrimer
Shore-D value	15	39	84	85

Table S4. The characteristics of the solar cells utilizing AgNW-GFRHybrimer films.

	Device 1	Device 2	Device 3	Device 4	Device 5	Average
PCE	5.50	5.74	5.41	5.35	5.90	5.58
J_{sc}	11.10	11.62	10.24	10.03	11.51	10.90
V_{oc}	0.88	0.87	0.87	0.86	0.85	0.86
FF	0.56	0.57	0.61	0.62	0.60	0.59

References

1 J. H. Jin, J. H. Ko, S. Yang, B. S. Bae, *Adv. Mater.* 2010, **22**, 4510.

2 The price of E-glass fabric (Nitto Boseki, Japan) is \$0.042/sheet (10 x 10 cm^2 in size).

3 On the basis of laboratory-level scale. In comparison, ITO/Glass (Samsung Corning Precision Materials, Korea), Eagle 2000 bare glass (Corning, Korea), and PET (Labtech, Korea) cost \$2.5, \$4.6, and \$1.2/sheet (10 x 10 cm^2 in size), respectively.

4 C. Yang, H. W. Gu, W. Lin, M. M. Yuen, C. P. Wong, M. Y. Xiong, B. Gao, *Adv. Mater.* 2011, **23**, 3052.

5 V. Scardaci, R. Coull, P. E. Lyons, D. Rickard, J. N. Coleman, *Small* 2011, **7**, 2621.

6 S. Sanchez, S. Berson, S. Guillerez, C. Levy-Clement, V. Ivanova, *Adv. Energy Mater.* 2012, **2**, 541.

7 S. C. Chien, F. C. Chen, M. K. Chung, C. S. Hsu, *J. Phys. Chem. C* 2012, **116**, 1354.